Check for updates

Manganese-ion Batteries

New Mn Electrochemistry for Rechargeable Aqueous Batteries: Promising Directions Based on Preliminary Results

Hyungjin Lee, Amey Nimkar, Hyeonjun Lee, Netanel Shpigel, Daniel Sharon, Seung-Tae Hong, and Munseok S. Chae*

Aqueous batteries with metal anodes exhibit robust anodic capacities, but their energy densities are low because of the limited potential stabilities of aqueous electrolyte solutions. Current metal options, such as Zn and Al, pose a dilemma: Zn lacks a sufficiently low redox potential, whereas Al tends to be strongly oxidized in aqueous environments. Our investigation introduces a novel rechargeable aqueous battery system based on Mn as the anode. We examine the effects of anions, electrolyte concentration, and diverse cathode chemistries. Notably, the ClO₄-based electrolyte solution exhibits improved deposition and dissolution efficiencies. Although stainless steel (SS 316 L) and Ni are stable current collectors for cathodes, they display limitations as anodes. However, using Ti as the anode resulted in increased Mn deposition and dissolution efficiencies. Moreover, we evaluate this system using various cathode materials, including Mn-intercalation-based inorganic (Ag_{0.33}V₂O₅) and organic (perylenetetracarboxylic dianhydride) cathodes and an anionintercalation-chemistry (coronene)-based cathode. These configurations yield markedly higher output potentials compared to those of Zn metal batteries, highlighting the potential for an augmented energy density when using an Mn anode. This study outlines a systematic approach for use in optimizing metal anodes in Mn metal batteries, unlocking novel prospects for Mn-based batteries with diverse cathode chemistries.

H. Lee, Prof. S.-T. Hong

Department of Energy Science and Engineering, DGIST, Daegu 42988, Korea

Department of Chemistry and BINA—BIU Centre for Nanotechnology and Advanced Materials, Bar Ilan University, Ramat Gan 5290002, Israel H. Lee, Prof. M. S. Chae

Department of Nanotechnology Engineering, Pukyong National University, Busan 48547, Korea

E-mail: mschae@pknu.ac.kr

Prof. N. Shpigel

Department of Chemical Sciences, Ariel University, Ariel 40700, Israel Prof. D. Sharon

Institute of Chemistry, The Hebrew University of Jerusalem, Jerusalem 9190401, Israel

Prof. S.-T. Hong

Department of Chemistry and Chemical Biology, University of New Mexico, Albuquerque, New Mexico 87131, USA

The ORCID identification number(s) for the author(s) of this article can be found under https://doi.org/10.1002/eem2.12823.

DOI: 10.1002/eem2.12823

1. Introduction

Aqueous batteries with H₂O-based electrolytes present a promising solution to safety concerns, and they exhibit versatile practicalities. Various iterations, including aqueous Li, Na, Mg, Ca, Al, NH₄-ion, and proton batteries, have emerged, each relying on a distinct charge carrier species. [1–6] However, their energy densities remain limited because of their nonmetallic anodes, fostering the excessive reliance on electrochemically inactive elements, such as current collectors and conductive additives. To overcome this limitation, the direct utilization of metals as anodes via plating/stripping mechanisms may optimize the anodic capacity and enhance efficiency.

Despite the progress in the use of metals, such as Cu, Fe, and Zn, as anodes, challenges persist, particularly concerning their poor plating/stripping potentials, which constrain the energy density, e.g. whereas aqueous Cu^[7] and Fe^[8] batteries exhibit high capacities, their operating potentials are relatively high (i.e. 0.34 and -0.45 V vs the standard hydrogen electrode [SHE], respectively), which practically

reduces their energy densities when coupled with positive cathodes. Aqueous Zn batteries struggle to higher potential of Zn because of its higher redox potential (-0.76 vs SHE) as an anode compared to that of Mn (-1.03 vs SHE). Al and Mg display lower plating/stripping potentials than that of Zn, but their low operating potentials and strong levels of passivation prevent their utilization in standard aqueous solutions. $^{[10-12]}$ Therefore, urgent exploration to identify metal anodes with lower plating/stripping potentials than those of Zn and the other materials is essential.

Mn has emerged as a promising candidate for use in high-energy aqueous batteries because of its high gravi—/volumetric capacity and low cost (**Figure 1**a). [8,13-19] In addition, in aqueous system, Mn exhibits a lower redox potential than that of Zn, and it theoretically displays a higher energy density than those of aqueous Zn battery systems (Figure 1b). Overall, Mn-based energy chemistry results in a reasonable aqueous system with a low cost and high stability and energy density (Figure 1c, and Table S1, Supporting Information). Yang et al. [20] fabricated an artificial passivation layer mediated by inorganic—organic electrolyte additives for reversible Mn deposition, but the efficient

1 of 6

electrochemistry was limited by the complex electrolyte composition. Our previous study focused primarily on the intercalation chemistry of Mn ions, and we successfully demonstrated Mn^{2+} intercalation into a Chevrel phase. Nevertheless, current research predominantly relies on MnCl_2 and MnSO_4 , lacking the exploration of diverse salts, current collector properties, and varied cathode chemistries for use in ion batteries. 14.21

This study introduces an innovative rechargeable aqueous battery based on Mn. We investigate the effects of various anions of salts, electrolyte concentrations, and cathode chemistries. Previous studies predominantly assessed process efficiency solely through mass discrepancies, rarely delving into its reversibility. So here, we underscore the insufficient understanding regarding how various electrolytes and current collectors influence the reversibility of the Mn deposition process. In addition, we demonstrate a hybrid battery concept based on anion intercalation and inorganic or organic electrodes based on Mn-ion intercalation. These findings highlight the broad potential of Mn batteries for use in future aqueous systems.

2. Results and Discussion

2.1. Aqueous Manganese Electrolyte and Anion/Concentration Effect

Considering the capacities of different anions to coordinate to metal cations, we first studied Mn anodes in the five most commonly used Mn-based electrolytes: MnSO₄, MnCl₂, Mn(NO₃)₂, Mn(CH₃CO₂)₂, and Mn(ClO₄)₂. All electrochemical tests were conducted using home-made three-electrode beaker-type cells. The electrochemical stability windows and deposition/dissolution behaviors of Mn were characterized using the electrolytes and a Pt mesh and working electrode with an area of 0.04 cm². To avoid potential unknown reactions, Pt electrode was employed. However, its hydrogen evolution reaction (HER) catalytic

(a) Gravimetric capacity 60000 300 40000 2000 Na ΑI Mn Zn Fe Gravimetric (b) (c) capacity Redox potential (V vs SHE) Affordabilit /olumetric SEI Stability Li Na Zn Mn

Figure 1. a) Gravi- and volumetric capacities and costs of typical metal anodes and b) the redox potentials of metal anodes. c) Radar plot of the performance properties of selected metal anodes.

properties pose limitations, particularly evident in the current collector aspect. As shown in Figure 2, at concentrations of 0.5 M, only electrolyte decomposition (the hydrogen evolution reaction (HER)) occurs, without noticeable Mn metal deposition (Figure 2a). However, at concentrations of 3 M in the same potential range, Mn metal deposition may be relatively favorable for certain salts. These high-concentration electrolytes suppress the HER. In addition, the Mn metal deposition is attributed to the molar concentration effect and desolvation energy between H₂O and the anions and Mn²⁺ ions. This behavior is potentially caused by the low charge densities of anions such as ClO₄, which facilitate Mn deposition in significant amounts (Figure 2b). The galvanostatic Mn//Mn symmetric cell also demonstrates for various electrolytes that the 3 M Mn(ClO₄)₂ electrolyte exhibits low deposition/dissolution voltage polarization with high efficiency (Figure S1, Supporting Information). Anodic stability is crucial on the cathode side (high-potential range), and evaluation with a Pt electrode reveals higher anodic stabilities in ClO₄-based electrolytes (Figure 2c).

Remarkably, upon increasing the concentration of the ClO₄⁻ electrolyte from 0.5 to 3 M, the Warburg slope increases sharply (Figure 2d,e). At low concentrations, the influence of ClO₄⁻ may be minimal due to the abundance of H₂O molecules.^[22] The aqueous 3 M Mn(ClO₄)₂ electrolyte exhibits a high deposition/dissolution Coulombic efficiency and reasonable anodic stability compared to those of the 3 M MnCl₂ electrolyte (after a few cycles, the efficiency suddenly declines), as shown in Figure 2f. The cycling details are provided in Figure S2, Supporting Information. Technically it is not high, but highest compared to the other electrolytes.

2.2. Manganese Electro-Deposition on Various Substrate

The number of Mn deposition/dissolution cycles of the Pt electrode is shown in **Figure 3**a. The current increases from the 1st to the 10th cycle, indicating an current activation of electrodeposition/dissolution

during cycles. We guess this activation process came from the increasing surface and catalytic properties from Mn or Mn(OH)2 which deposited in previous cycles. Moreover, a decrease in resistance during dissolution is apparent, based on the reduction in the peak potential from -0.88 to -0.98 V (vs Ag/AgCl) in the cyclic voltammogram. With each cycle, Mn or Mn(OH)2 electrodeposition increases in activity (-1.4 V vs Ag/AgCl), yet HER activation is also observed at approximately -1.3 V(vs Ag/AgCl). Figure 3b shows the anodic stabilities of the 3 M Mn(ClO₄)₂ electrolyte on various current collectors. Al and Cu induce instability, whereas Ni and stainless steel (SS 316 L) induce stability at higher potentials. Additionally, when the Mn deposition/dissolution cycle is conducted using various metals as anodes, unexpectedly, Ni and SS 316 L exhibit lower efficiencies due to corrosion. Conversely, Pt and Ti display the highest stabilities, with coulombic efficiencies of approximately 40%, indicating the coexistence of HER reactions within the electrolyte (Figure 3c, Figures S3 and \$4, Supporting Information).

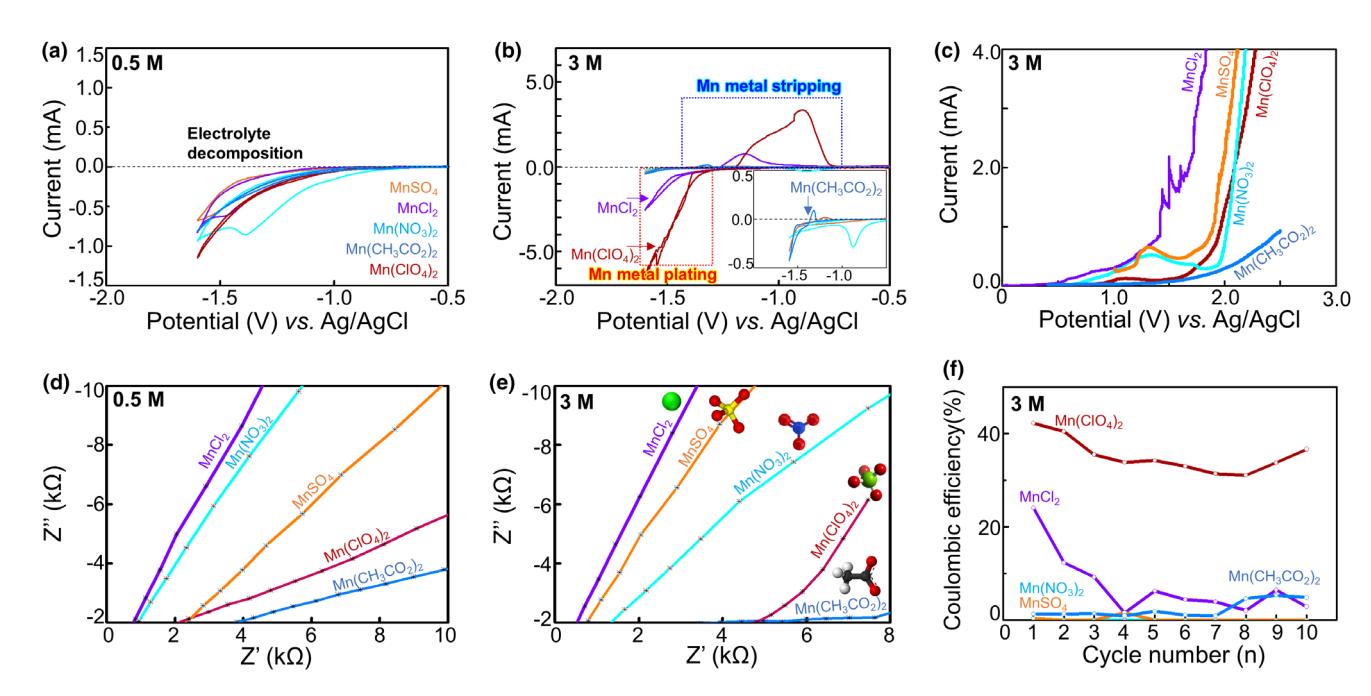


Figure 2. Mn metal plating on the Pt electrode with aqueous a) 0.5 and b) 3 M MnCl₂, MnSO₄, Mn((NO)₃)₂, Mn(ClO₄)₂, and Mn(CH₃CO₂)₂ electrolytes (scan rate: 20 mV s⁻¹). c) Anodic stabilities of the 3 M electrolytes. Impedance slopes of the d) 0.5 and e) 3 M electrolytes. f) Coulombic efficiencies in various 3 M Mn electrolyte solutions at 293 K.

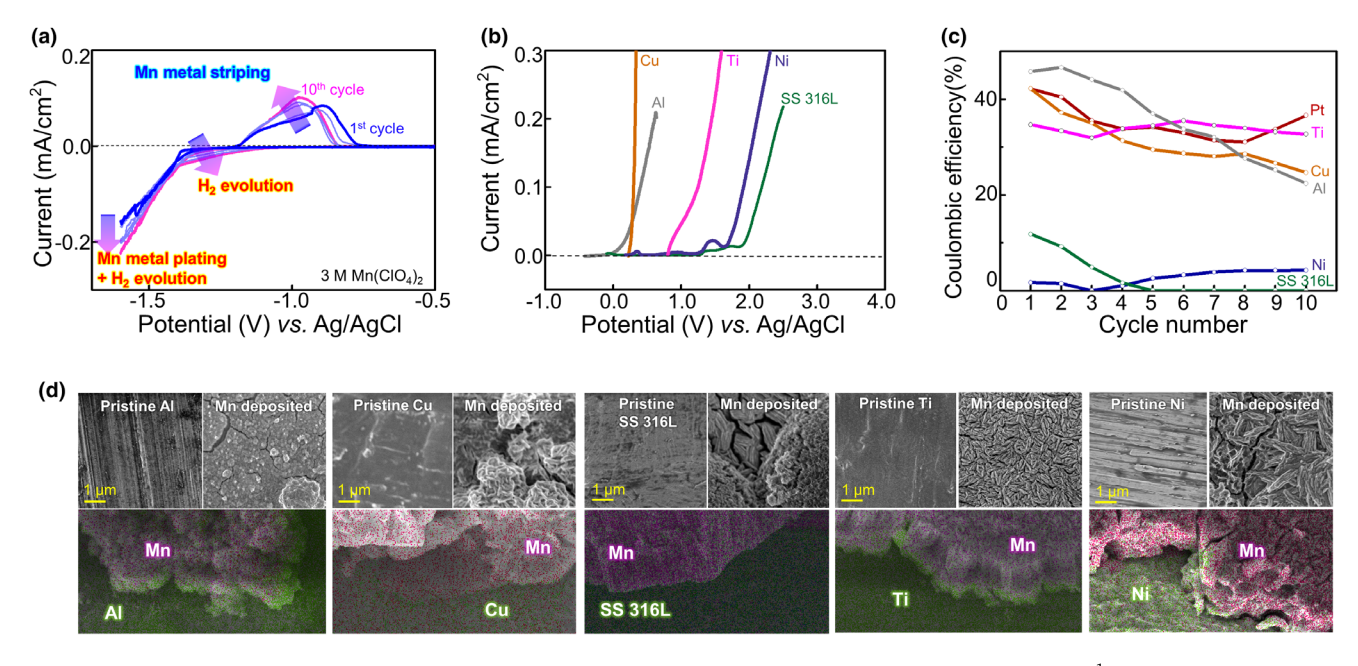


Figure 3. a) Cycles of Mn metal plating on the Pt electrode with the aqueous 3 M $Mn(ClO_4)_2$ electrolyte (scan rate: 20 mV s⁻¹). b) Anodic stabilities of the aqueous 3 M $Mn(ClO_4)_2$ electrolyte on various substrates. c) Coulombic efficiencies at room temperature. d) SEM–EDX images of Mn plating on various substrates.

Thus, future studies should address the stability concerns by incorporating organic electrolyte additives. Another aspect of the use of metal anodes is dendrite formation, and thus, we examined the morphology after Mn deposition. The variation in the obtained Mn morphology with respect to the selected substrate is clearly visible in the scanning electron microscopy-energy-dispersive X-ray spectroscopy (SEM–EDX)

images shown in Figure 3d. Randomly arranged Mn crystals are formed on the Al, Cu, SS 316 L, and Ni substrates, whereas mixtures of aggregated Mn clusters and vertically oriented crystals are observed on the electroplated SS 316 L foils (Figures S5–S9, Supporting Information). As a result, titanium foil offers uniform electroplating in $Mn(ClO_4)_2$ aqueous electrolyte, possibly due to two reasons. 1) The $Mn(ClO_4)_2$

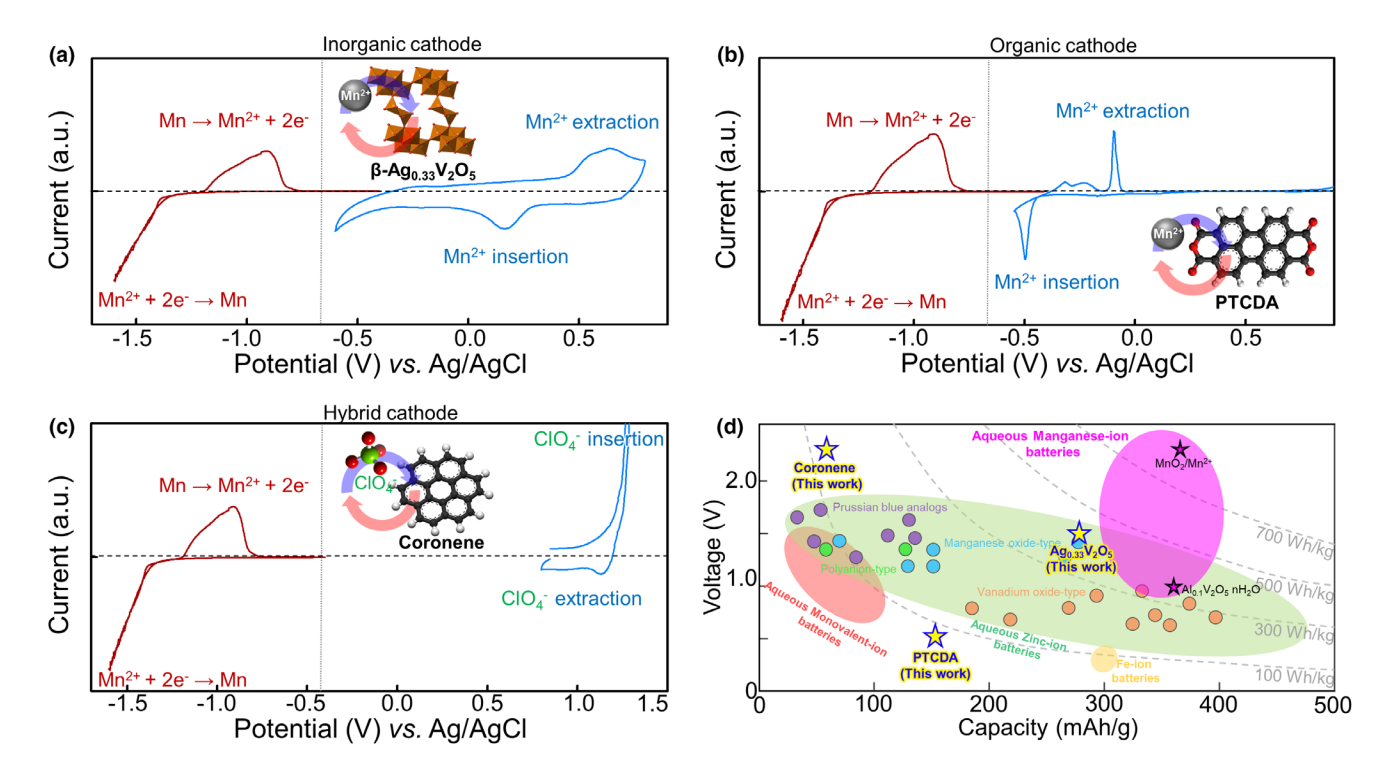


Figure 4. Cyclic voltammograms of the Mn anode (red) at 20 mV s⁻¹ and the various cathodes (blue) at 0.3 mV s⁻¹ in stable aqueous 3 M Mn(ClO₄)₂ electrolytes: a) Mn intercalation chemistry within the inorganic β-Ag_{0.33}V₂O₅ structure, b) Mn redox chemistry on the organic PTCDA structure, and c) anion intercalation chemistry within the organic coronene structure (hybrid battery system). d) Discharge capacities for manganese battery cathodes and potentials of various aqueous battery systems.

based electrolyte's pH is not strongly acidic, preventing the promotion of the HER reaction and allowing for stable electrodeposition. 2) The type and structural orientation of the metal can influence the deposition tendency due to the metal's surface energy and catalytic properties. This phenomenon also observed in zinc metal plating research^[23].

On the Ti substrate, plate-like Mn crystals oriented perpendicular to the surface are observed. When Mn is electrodeposited on a Ti substrate, smooth (and uniform) deposition occurs without significant dendrite formation, resulting in shapes with sizes of approximately 300 nm (Figure S9, Supporting Information). After Mn electrodeposition on Ti foil, we conducted XRD measurements. The electrochemically deposited Mn metals underwent oxidation to the MnO2 phase during XRD analysis in the air condition. However, Mn(OH)2 still persisted in the XRD results, which may contribute to lower coulombic efficiency [24] (Figure S10, Supporting Information). These results indicate that Mn metal deposition and Mn(OH)2 formation occur during electrodeposition, with only Mn undergoing oxidation (as Mn metal stripping, see Figure 3a). Unfortunately, direct evidence of Mn electrodeposition cannot be observed in the common XRD technique due to oxidation from water HER reaction or oxygen from the air. To clearly observe this phenomenon, in-situ XRD may be needed and it will be covered future scope of the study.

2.3. Various Cathode Chemistries for Manganese Battery

Due to the potential of ion batteries as aqueous systems, various studies are in their preliminary stages. One such system is the bilayered structure based on intercalation reactions, which is represented by vanadium

oxides, such as $Mn_{0.18}V_2O_5 \cdot nH_2O^{[21]}$ and $Al_{0.1}V_2O_5 \cdot 1.5H_2O^{[16]}$. Additionally, batteries comprising Chevrel phases and Prussian blue analogues have been implemented, and furthermore^[15], a battery utilizing the Mn/MnO_2 redox reaction was developed^[14]. However, these Mn-ion batteries may be used to explore a wider range of chemistries.

First, we demonstrated an $Ag_{0.33}V_2O_5$ structure utilizing Mn-ion intercalation and chemical displacement reactions. The synthesized $Ag_{0.33}V_2O_5$ was confirmed by Rietveld refinement (Figure S11, Supporting Information). The redox reactions of Mn metal and the Mn storage reaction of $Ag_{0.33}V_2O_5$ are shown in red and blue, respectively, in **Figure 4a**. When we utilized Mn metal as anode, an energy density in an aqueous environment that is approximately 0.6 V higher than the redox potentials in conventional Zn secondary batteries. Using internal ions, such as Cu or Ag, may further enhance the capacity via chemical substitution reactions (Figures S12 and S13, Supporting Information). Their detailed electrochemical data are attached in Figure S14, Supporting Information. The discharge capacity of $Ag_{0.33}V_2O_5$ shows 261.9 mAh g^{-1} at a current of 100 mA g^{-1} . this structure also possible to accommodate the proton from the aqueous electrolyte. The clear reaction mechanism will be covered in further scope of the study.

Second, the application of organic electrode materials is due to their facile redox reactions, which offer several advantages, such as faster kinetics, higher capacities, and low costs. ^[25] Thus, we utilized one of the most widely used organic dyes, i.e. perylenetetracarboxylic dianhydride (PTCDA), as an electrode, confirming its reversible reaction within a range of approximately 1 V (Figure 4b). The PTCDA powder was confirmed by Rietveld refinement (Figure S15, Supporting Information). PTCDA undergoes a facile redox reaction with Mn²⁺ ions, as indicated by the sharp redox couple observed in the cyclic

voltammogram. Various organic electrodes may be stably operated in aqueous systems, and Mn ions may be stored via Mn-carbonyl bonding, in addition to π -electron bonding. We propose the exploration of the potentials of various organic cathode materials (Figure S16, Supporting Information). The detailed electrochemical data of PTCDA electrode are attached in Figure S17, Supporting Information.

Finally, anion intercalation reactions (like graphite) were explored using the polycyclic compound coronene.^[27] The coronene powder was confirmed by Rietveld refinement (Figure S18, Supporting Information). Figure 4c shows the cyclic voltammograms of the coronene cathode. Coronene successfully displays ClO₄ storage, but this includes the oxygen evolution reaction. The MnOOH and MnO2 generation are excluded in this reaction, only Cl peaks are detected in charged sample it suggested that ClO₄ is inserted in to coronene structure (Figure \$19, Supporting Information). This indicates the feasibility of realizing potentials of up to ~2.5 V while maximizing the stability range of the electrolyte in an aqueous solution. In addition, the introduction of wet organic electrolytes may yield higher potentials. This study utilizes ClO₄ anions, but similar to various anion chemistries used previously, this suggests the potential of employing a diverse range of anions in Mn-ion battery systems. The detailed electrochemical data of coronene electrode are attached in Figure \$20, Supporting Information. Nevertheless, the voltage range exceeding 1.2 V versus Ag/ AgCl renders water splitting (irreversible) and the oxidation of Mn²⁺ to MnO₂ feasible in aqueous manganese electrolyte. Hence, the efficacy of anion insertion chemistry in the manganese aqueous system may be limited. However, the utilization of organic-based electrolytes could warrant reconsideration.

These systems were compared with Zn-based and other aqueous battery systems, as shown in Figure 4d. Zn-based batteries display the most promising energy densities among those of aqueous battery systems. However, upon using an Mn metal anode, the operating potential increases by approximately 0.6 V, indicating the possibility of surpassing conventional Zn-ion secondary batteries in the field of aqueous battery systems.

In this research, we designed a battery mainly using aqueous electrolytes to assume that manganese ion batteries are inexpensive. However, we discovered a fundamental decrease in electrodeposition efficiency due to the formation of $Mn(OH)_2$ and the HER reaction. Therefore, for future research directions, we consider the surface coating to reduce overpotential, [28] organic electrolytes, and organic salt, which can be used singly or in combination. [29] Recently, research on cathode deposition using organic electrolytes and halide salts has been reported. [30] However, fundamentally, halide salts can cause corrosion. Therefore, research on alternative salts is also considered for the further scope of the study. In addition to achieving uniform manganese electrodeposition without other phases using an aqueous solution, pH adjustment is also an important factor in decreasing the $Mn(OH)_2$ phase.

3. Conclusion

In conclusion, this study introduces a promising rechargeable aqueous battery technology that uses Mn as an anode. We extensively analyzed the influences of anions, electrolyte concentrations, and diverse cathode chemistries. Notably, the ${\rm ClO_4}^-$ based electrolyte exhibited superior deposition and dissolution efficiencies owing to its chaotropic nature. Although SS 316 L and Ni were stable current collectors for cathodes, they exhibited limitations as anodes. In contrast, the use of Ti as the

anode resulted in an enhanced Mn deposition/dissolution efficiency and anti-dendrite formation effects. Additionally, we evaluated this system using a range of cathode materials, including Mn-intercalationand chemical displacement-based inorganic (e.g. $Ag_{0.33}V_2O_5$) and organic (PTCDA) cathodes, in addition to an anion-intercalation-chemistry (coronene)-based cathode. These configurations yielded significantly higher output potentials compared to those of Zn metal batteries, indicating the potential for increased energy density by utilizing an Mn anode. This investigation delineates a systematic approach for use in optimizing efficient Mn metal anodes in Mn metal batteries, unlocking novel opportunities for Mn-based batteries with diverse cathode chemistries.

4. Experimental Section

Detailed information related to the synthesis of active electrodes, physicochemical characterization, and electrochemical evaluation of bifunctional electrodes towards UOR and supercapacitor application is provided in Supporting Information.

Acknowledgements

This work was supported by the Global Joint Research Program funded by the Pukyong National University (202411790001).

Conflict of Interest

The authors declare no conflict of interest.

Supporting Information

Supporting Information is available from the Wiley Online Library or from the author.

Keywords

anion effect, cathode materials, current collectors, manganese batteries, manganese electrolytes

Received: April 22, 2024 Revised: June 21, 2024 Published online: July 17, 2024

- M. S. Chae, H. J. Kim, J. Lyoo, R. Attias, Y. Elias, Y. Gofer, S.-T. Hong, D. Aurbach, ACS Appl. Energy Mater. 2020, 3, 10744.
- [2] R. Emanuelsson, M. Sterby, M. Strømme, M. Sjodin, J. Am. Chem. Soc. 2017, 139, 4828.
- [3] S. Gheytani, Y. Liang, F. Wu, Y. Jing, H. Dong, K. K. Rao, X. Chi, F. Fang, Y. Yao, Adv. Sci. 2017, 4, 1700465.
- [4] L. Suo, O. Borodin, W. Sun, X. Fan, C. Yang, F. Wang, T. Gao, Z. Ma, M. Schroeder, A. von Cresce, Angew. Chem. 2016, 128, 7252.
- [5] F. Wang, X. Fan, T. Gao, W. Sun, Z. Ma, C. Yang, F. Han, K. Xu, C. Wang, ACS Central Sci. 2017, 3, 1121.
- [6] X. Wu, Y. Qi, J. J. Hong, Z. Li, A. S. Hernandez, X. Ji, Angew. Chem. Int. Ed. 2017, 56, 13026.
- [7] G. Liang, F. Mo, Q. Yang, Z. Huang, X. Li, D. Wang, Z. Liu, H. Li, Q. Zhang, C. Zhi, Adv. Mater. 2019, 31, 1905873.

- [8] X. Wu, A. Markir, Y. Xu, C. Zhang, D. P. Leonard, W. Shin, X. Ji, Adv. Funct. Mater. 2019, 29, 1900911.
- [9] C. Xu, B. Li, H. Du, F. Kang, Angew. Chem. 2012, 124, 957.
- [10] G. A. Elia, K. V. Kravchyk, M. V. Kovalenko, J. Chacón, A. Holland, R. G. Wills, J. Power Sources 2021, 481, 228870.
- [11] H. D. Yoo, I. Shterenberg, Y. Gofer, G. Gershinsky, N. Pour, D. Aurbach, Energ. Environ. Sci. 2013, 6, 2265.
- [12] D. Aurbach, Z. Lu, A. Schechter, Y. Gofer, H. Gizbar, R. Turgeman, Y. Cohen, M. Moshkovich, E. Levi, *Nature* 2000, 407, 724.
- [13] M. Wang, X. Zheng, X. Zhang, D. Chao, S. Z. Qiao, H. N. Alshareef, Y. Cui, W. Chen, Adv. Energy Mater. 2021, 11, 2002904.
- [14] M. Wang, Y. Meng, Y. Xu, N. Chen, M. Chuai, Y. Yuan, J. Sun, Z. Liu, X. Zheng, Z. Zhang, Energ. Environ. Sci. 2023, 16, 5284.
- [15] A. Nimkar, M. S. Chae, S. Wee, G. Bergman, B. Gavriel, M. Turgeman, F. Malchik, M. D. Levi, D. Sharon, M. R. Lukatskaya, ACS Energy Lett. 2022, 7, 4161.
- [16] S. Bi, Y. Zhang, S. Deng, Z. Tie, Z. Niu, Angew. Chem. Int. Ed. 2022, 61, e202200809.
- [17] N. Yabuuchi, K. Kubota, M. Dahbi, S. Komaba, Chem. Rev. 2014, 114, 11636.
- [18] G. A. Elia, K. Marquardt, K. Hoeppner, S. Fantini, R. Lin, E. Knipping, W. Peters, J.-F. Drillet, S. Passerini, R. Hahn, Adv. Mater. 2016, 28, 7564.
- [19] J. Tu, W. L. Song, H. Lei, Z. Yu, L. L. Chen, M. Wang, S. Jiao, Chem. Rev. 2021, 121, 4903.

- [20] Q. Yang, X. Qu, H. Cui, X. He, Y. Shao, Y. Zhang, X. Guo, A. Chen, Z. Chen, R. Zhang, Angew. Chem. Int. Ed. 2022, 61, e202206471.
- [21] S. Bi, S. Wang, F. Yue, Z. Tie, Z. Niu, Nat. Commun. 2021, 12, 6991.
- [22] A. Nimkar, K. Alam, G. Bergman, M. D. Levi, D. T. Major, N. Shpigel, D. Aurbach, Angew. Chem. Int. Ed. 2023, 135, e202311373.
- [23] S. Zhou, X. Meng, Y. Chen, J. Li, S. Lin, C. Han, X. Ji, Z. Chang, A. Pan, Angew. Chem. Int. Ed. 2024, 136, e202403050.
- [24] Z. Cheng, Q. Dong, G. Pu, J. Song, W. Zhong, J. Wang, Small 2024, 20, 2400389.
- [25] A. Nimkar, G. Bergman, E. Ballas, N. Tubul, N. Levi, F. Malchik, I. Kukurayeve, M. S. Chae, D. Sharon, M. Levi, Angew. Chem. 2023, 135, e202306904.
- [26] M. S. Chae, A. Nimkar, N. Shpigel, Y. Gofer, D. Aurbach, ACS Energy Lett. 2021, 6, 2659.
- [27] I. A. Rodríguez-Pérez, Z. Jian, P. K. Waldenmaier, J. W. Palmisano, R. S. Chandrabose, X. Wang, M. M. Lerner, R. G. Carter, X. Ji, ACS Energy Lett. 2016, 1, 719.
- [28] Y. Feng, N. Ran, X. Wang, Q. Liu, J. Wang, L. Liu, K. Suenaga, W. Zhong, R. Ma, J. Liu, Adv. Energy Mater. 2023, 13, 2302452.
- [29] X. Wang, R. Ma, S. Li, M. Xu, L. Liu, Y. Feng, T. Thomas, M. Yang, J. Wang, Adv. Energy Mater. 2023, 13, 2300765.
- [30] D. Shen, X. Zheng, R. Luo, T. Jiang, M. Wang, M. Zhang, Q. Peng, L. Song, S. Zhou, Z. Hou, Y. Qian, W. Chen, Joule 2024, 8, 780.